Original Article

Genomic analysis of the endosomal sorting required for transport complex III pathway genes as therapeutic and prognostic biomarkers for endometrial carcinoma

Ye Yang[1]^, Min Wang[2]

[1]Obstetrics and Gynecology Department, Shanghai General Hospital, Shanghai Jiao Tong University School of Medicine, Shanghai, China; [2]General Surgery Department, Shanghai General Hospital, Shanghai Jiao Tong University School of Medicine, Shanghai, China

Contributions: (I) Conception and design: Y Yang; (II) Administrative support: Y Yang; (III) Provision of study materials or patients: Y Yang; (IV) Collection and assembly of data: Both authors; (V) Data analysis and interpretation: Both authors; (VI) Manuscript writing: Both authors; (VII) Final approval of manuscript: Both authors.

Correspondence to: Min Wang. Department of General Surgery, Shanghai General Hospital, Shanghai Jiao Tong University School of Medicine, 85 Wujin Road, Hongkou, Shanghai 200080, China. Email: wangmin0501@hotmail.com.

Background: The genes involved in the endosomal sorting required for transport complex (ESCRT)-III pathway is a protective mechanism that delays cell death by repairing damaged plasma membranes. We aimed to evaluate if targeting *ESCRT-III* genes may be used as biomarkers for predicting the clinical outcomes of endometrial carcinoma (EC).

Methods: Transcriptome RNA sequence (RNA-seq) data and genomic information of EC samples were obtained from The Cancer Genome Atlas (TCGA). The expression level, pathological relationship, pathway alterations, mutation, functional enrichment, associations with tumor infiltrating lymphocytes (TILs), and survival information of *ESCRT-III* genes including charged multivesicular body protein 2A (*CHMP2A*), *CHMP2B*, *CHMP3*, *CHMP4B*, *CHMP4C*, *CHMP5*, *CHMP5*, and *CHMP7* in EC and normal tissues were explored through multiple datasets analysis.

Results: Our study demonstrated that *CHMP2B*, *CHMP3*, *CHMP4B*, *CHMP5*, *CHMP5*, and *CHMP7* were significantly lower, whereas *CHMP2A* and *CHMP4C* were significantly higher in EC tissue than in normal tissue. All ESCRT pathway genes were significantly differentially expressed between tumor grades 2 and 3 and were positively correlated with each other. Except for *CHMP5*, the other seven ESCRT pathway genes were the most frequently mutated genes in the EC samples among all cancer types. Moreover, *CHMP2A* and *CHMP7* had better prognostic potential in EC. *CHMP2A*, *CHMP4B*, and *CHMP7* were significantly correlated with all four molecular subtypes in TCGA. Increased expression of *CHMP2A* and *CHMP7* and decreased expression of *CHMP4B* were observed in EC samples than in serous carcinoma type samples. Furthermore, they were associated with tumor stages 1 and 2 and good survival outcomes for EC. Functional analysis revealed that the *ESCRT-III* genes were involved in the biological process (BP) of the membrane budding and multivesicular body (MVB) pathway; *CHMP2A* and *CHMP7* participated in the ESCRT and ESCRT III complex disassembly, while *CHMP5* was involved in ESCRT and ESCRT III complex assembly.

Conclusions: Mutations in *CHMP2A* and *CHMP7* correspond to a better prognostic potential in EC. Upregulation of *CHMP2A* and *CHMP7* and downregulation of *CHMP4B* are good prognostic indicators of the histological type, early tumor grade, and promising survival markers, thus becoming potential biomarkers and therapeutic targets for EC.

Keywords: *ESCRT-III*; *CHMP2A*; *CHMP4B*; *CHMP7*; endometrial carcinoma (EC)

^ ORCID: 0000-0002-4180-2822.

Submitted Mar 11, 2022. Accepted for publication Jul 08, 2022.
doi: 10.21037/tcr-22-660
View this article at: https://dx.doi.org/10.21037/tcr-22-660

Introduction

Endometrial carcinoma (EC) is one of the most common gynecological cancers worldwide, with an estimated new cases and deaths of 65,950 and 12,550, respectively (1). EC has two subgroups, namely, types I and II. Type I is characterized by an upregulation of hormonal receptors. It consists of 60–70% of EC and histological grades 1 and 2. Type II is characterized by low levels of estrogen and progesterone receptor expression. Moreover, it is associated with high-grade EC and serous or clear cell carcinoma with poor prognosis (2). After surgical resection, chemotherapy and radiotherapy for EC, the 5-year disease-free survival (DFS) of patients diagnosed in the early stages, stages III or IV, and recurrent or metastatic disease decreased progressively to 74.2–90.8%, 57.3–66.2%, 20.1–25.5%, and 16%, respectively (3). Targeted therapies for tyrosine kinases and immunotherapy using immune-checkpoint inhibitors (4) are clinical strategies used in cancer treatment. These modalities aim to kill tumor cells and protect normal cells.

The endosomal sorting required for transport complex III (*ESCRT-III*) acts as a protective mechanism that delays cell death by repairing damaged plasma membranes due to necroptosis (5), pyroptosis (6), and ferroptosis (7). The *ESCRT-III* complex incorporates charged multivesicular body protein 2A (*CHMP2A*), *CHMP2B*, *CHMP3*, *CHMP4B*, *CHMP4C*, *CHMP5*, *CHMP5*, and *CHMP7*, which belong to the chromatin-modifying protein/charged multivesicular body protein (CHMP) family (8) (Figure S1). These are involved in the MVB sorting pathway and are important in recycling and degradation of membrane proteins. ESCRT-I, ESCRT-II, and *ESCRT-III*, as well as VPS4A and ALIX were triggered by $Ca2^{+}$ influx, recruited to damaged lysosomes and mediated lysosomal membrane repair (8). Detailed information on the location and synonyms of these eight *ESCRT-III* genes is listed in Tables S1,S2. Since regulated cell death usually occurs in drug resistant tissues during EC therapy (9), we aimed to determine whether *ESCRT-III* genes might function as potential targets in the treatment and prognosis of EC.

Searching for tumor genomic biomarker using microarray RNA sequencing (RNA-Seq) data was recently applied to determine cancer prognosis. In this study, we performed bioinformatics technology with a high-throughput screening data to identify the *ESCRT-III* pathway gene signature in EC using the UALCAN, Clinical Proteomic Tumor Analysis Consortium (CPTAC) Confirmatory/Discovery, TISIDB, Gene Expression Profiling Interactive Analysis (GEPIA), and NIH National Cancer Institute CDC Data Portal dataset on the uterine corpus endometrial carcinoma (UCEC) dataset of the Cancer Genome Atlas (TCGA) database. Data on gene expression profiles, pathological relationship, somatic mutation status, function enrichment pathway, correlation with tumor infiltrating lymphocytes (TILs), and survival analysis were generated to assess if *ESCRT-III* pathway genes could be regarded as potential therapeutic targets and candidate prognostic biomarkers for EC. We present the following article in accordance with the STREGA reporting checklist (available at https://tcr.amegroups.com/article/view/10.21037/tcr-22-660/rc).

Methods

Acquisition of data on ESCRT-III pathway genes

This study conformed to the provisions of the Declaration of Helsinki (as revised in 2013). Data on the transcriptional levels of over- and under-expressed ESCRT pathway genes as determined by Transcriptome RNA sequence (RNA-Seq) analysis were collected using the UALCAN analysis (http://ualcan.path.uab.edu) (EC: 546; normal: 35) (10) from the UCEC dataset of the TCGA database (https://portal.gdc.cancer.gov/). We also conducted GEPIA (http://gepia.cancer-pku.cn/) (11) for data mining and visualization of the RNA sequencing expression data to validate the expression profiles of the ESCRT pathway genes in UCEC primary tumors (n=174) from TCGA-UCEC and GTEx-Uterus projects (12). The matched TCGA normal and GTEx data were combined into the normal group (n=91). The default parameters were $|Log_2FC|$ Cutoff of 1, P value cutoff of 0.01, and log2 (transcripts per million, TPM +1) for log-

scale were used. A jitter size of 0.4 was generated. Z-values representing standard deviations from the median across EC and normal endometrial tissue samples were identified using the Clinical Proteomic Tumor Analysis Consortium (CPTAC) Confirmatory/Discovery dataset (http://ualcan.path.uab.edu/analysis-prot.html) (13) (EC: 100; normal: 31) and normalized by Log2 spectral count ratio values both in each sample profile and across samples.

Clinical pathological relationship and pathway analyses of the ESCRT genes

The relationship between ESCRT genes and basic clinical pathological information, including subtype, tumor grade, histology, individual cancer stages, and methylation status, were further explored using the UALCAN and CPTAC datasets. We systematically assessed the ESCRT genes involved in key pathways across EC samples based on the CPTAC dataset, which were represented by Z-values. Associations of the *ESCRT-III* pathway gene expression and immune/molecular subtypes across EC analyzed using the Kruskal-Wallis Test -log10(P value) were identified on the TISIDB (http://cis.hku.hk/TISIDB/index.php) (14) dataset.

Function enrichment and pathway analyses of the ESCRT pathway genes

To obtain the enriched biological functions and pathways of the ESCRT pathway genes, we conducted the Gene Ontology (GO) and Kyoto Encyclopedia of Genes and Genomes (KEGG) analyses on TISIDB. Statistical significance was set at $P<0.05$. Connections among the ESCRT pathway gene expression were analyzed via the Pearson's correlation on the GEPIA dataset.

Validation of ESCRT gene mutations in the EC samples

We obtained the mutation data on the ESCRT pathway genes in the TCGA-UCEC cohort from the NIH National Cancer Institute GDC Data Portal database (https://portal.gdc.cancer.gov). We calculated the number of cases of ESCRT genes affected by simple somatic mutation (SSM) across the TCGA project (n=530). Cases affected by copy number variation (CNV) gains and losses in the TCGA database (n=510) were also analyzed computationally. Disease type in the UCEC project included adenomas, adenocarcinomas, cystic, mucinous, serous, and epithelial neoplasms. Statistical calculations of mutation types, including somatic mutations, CNV losses, CNV gains, SSM affected, variant effect predictor (VEP) impact mutation, Sorting Intolerant From Tolerant (SIFT) impact mutation, Polyphen Impact Mutation, Consequence Type Mutation, Type Mutation and Variant Caller Mutation were obtained and listed in Table S3. The frequency and pathogenicity of the variants in the exons were determined using bioinformatic prediction tools. We also gathered the clinical survival time and status of the EC patients.

Association between gene expression and TILs

We utilized the online tools, TISIDB and GEPIA2021 (http://gepia2021.cancer-pku.cn/sub-expression.html), based on the TCGA database using Spearman correlations to investigate the correlations between genes and their immune microenvironment (15). The relative abundance of 28 TIL types was determined using gene set variation analysis (GSVA) based on gene expression profiles (16).

Survival analysis

To screen the relationship between the expression profiles of the ESCRT pathway genes and the overall survival (OS) between high- and low-expression groups from the TCGA-UCEC dataset, we inferred the Kaplan-Meier survival curves on UALCAN [N (high *vs.* low/medium) =137 *vs.* 408] and TISDB analysis. Genes with a statistical significance, as determine by conducting the log-rank test ($P<0.05$), were considered prognostic genes of EC. We also carried out a univariate Cox proportional hazards regression analysis in GEPIA with EC samples that had high and low expression levels in 86 cases from the TCGA to evaluate their OS and DFS. The Cox proportional hazard ratio (HR) was based on the Cox PH model, while the 95% confidence interval (CI) was included in the survival plot as a dotted line. The median expression threshold for splitting the high- and low-expression cohorts as group cutoff was established. Patients who exhibited an upregulation showed expression values > third quartile. They were then divided into high- or low-expression groups with a median group cutoff of 50%. ESCRT gene mutations associated with survival rates were collected.

Statistical analysis

RNA-seq expression of the TPM of ESCRT pathway genes in the TCGA-UCEC and GTEx-Uterus data,

clinicopathological relationships, and pathways were analyzed via ANOVA. The ESCRT pathway genes associated with immune and molecular subtypes were analyzed using the Kruskal-Wallis test -log10(P value). The Chi-square and the Fisher's exact tests were used to compare the mutations. The Spearman's correlation test was used to explore the correlation between gene expression levels and the immune cell types. The Kaplan-Meier survival curves were used to analyze the OS, and univariate Cox proportional hazards regression analysis was used to evaluate the OS and DFS. The statistical significance was set at $P<0.05$.

Online database

The online databases were as follows: TCGA (https://portal.gdc.cancer.gov/); UALCAN (http://ualcan.path.uab.edu) (10); TISIDB (http://cis.hku.hk/TISIDB/index.php (14); GEPIA: Gene Expression Profiling Interactive Analysis (http://gepia.cancer-pku.cn/) (11); GEPIA2021 (http://gepia2021.cancer-pku.cn/sub-expression.html; CPTAC Confirmatory/Discovery dataset (http://ualcan.path.uab.edu/analysis-prot.html) (13); and NIH National cancer institute CDC Data Portal database (https://portal.gdc.cancer.gov).

Results

Validation of the ESCRT-III pathway genes in EC samples

We investigated the transcriptional RNA expression levels of the key genes in the *ESCRT-III* pathway in EC and normal endometrial tissues. *CHMP2B*, *CHMP5*, *CHMP5*, and *CHMP7* were significantly lower, while *CHMP2A* and *CHMP4C* were significantly higher in EC samples (n=546) than in normal endometrial samples (n=35) in the UALCAN analysis of the TCGA-UCEC database (Figure S2A, Table S4). We also verified the expression values of the ESCRT genes by conducting the GEPIA analysis, which indicated a significantly higher expression level of *CHMP4C* in the EC samples (n=174) than in the normal samples (n=91) on the TCGA-UCEC and GTEx-Uterus data (n=13). Genes, such as *CHMP2A*, *CHMP4B*, and *CHMP5*, have higher levels of expression (Figure S2B, Table S4). On the other hand, *CHMP2B*, *CHMP3*, *CHMP5* and *CHMP7* had lower levels of expression in the EC samples. In addition, differential analysis through CPTAC characterized by Z-values revealed that *CHMP2A*, *CHMP2B*, *CHMP3*, and *CHMP4B* were markedly lower in the EC samples (n=100) and normal endometrial tissues (n=31), whereas *CHMP4C* and *CHMP5* showed significantly higher differences in EC samples (Figure S2C, Table S4). *CHMP2A* had a higher level of expression on the UALCAN dataset than on the CPTAC. *CHMP5* had a significantly lower expression on the UALCAN dataset than on the CPTAC. This may possibly be due to different sample sizes and comparison methods with transcriptional RNA expression levels on UALACN, GEPIA, and the Z-value of standard deviations on CPTAC.

Analysis of the clinical pathological characteristics of the ESCRT-III pathway genes in EC samples

We further compared the expression profiles of ESCRT pathway genes in different tumor stages, grades, subtypes, histological/immune/molecular subtypes, TP53 mutants, methylation, and pathways altered on the TCGA-UCEC and GTEx-Uterus datasets in the UALCAN, CPTAC, and TISDIB analyses, respectively. In the UALCAN analysis, *CHMP2A*, *CHMP2B*, *CHMP4C*, *CHMP5*, and *CHMP7* were significantly differentially expressed among the International Federation of Gynecology and Obstetrics (FIGO) stages 1 to 3 and the normal sample. Different analyses revealed a significantly increased expression of *CHMP2A*, *CHMP4C*, and *CHMP7*, as well as decreased expression of *CHMP2B* and *CHMP5* in endometrioid and serous carcinoma samples compared with normal samples. In addition, *CHMP2A*, *CHMP4B*, *CHMP5*, and *CHMP7* were significantly different between the endometrioid and serous carcinoma samples. An increase in the expression of *CHMP2A* and *CHMP7* and a decrease in the expression of *CHMP4B* were observed in the EC samples compared with the serous carcinoma samples. *CHMP2A*, *CHMP4B*, *CHMP4C*, *CHMP5*, and *CHMP7* were significantly associated with TP53 mutation status in EC samples. Moreover, we found that the methylation status of *CHMP2A*, *CHMP2B*, *CHMP4C*, and *CHMP5* was strongly correlated with their expression levels (*Figure 1A*, Table S4). In summary, we found that *CHMP2B*, *CHMP3*, *CHMP4B*, *CHMP5*, and *CHMP7* were significantly downregulated, while *CHMP2A*, *CHMP4C* were significantly upregulated in the EC samples.

In the CPTAC analysis, all ESCRT pathway genes were significantly differentially expressed between histologic grades 2 and 3. *CHMP2A*, *CHMP2B*, *CHMP3*, *CHMP4B*, and *CHMP4C* were significantly differentially expressed between grade 1, grade 2, and normal samples. To

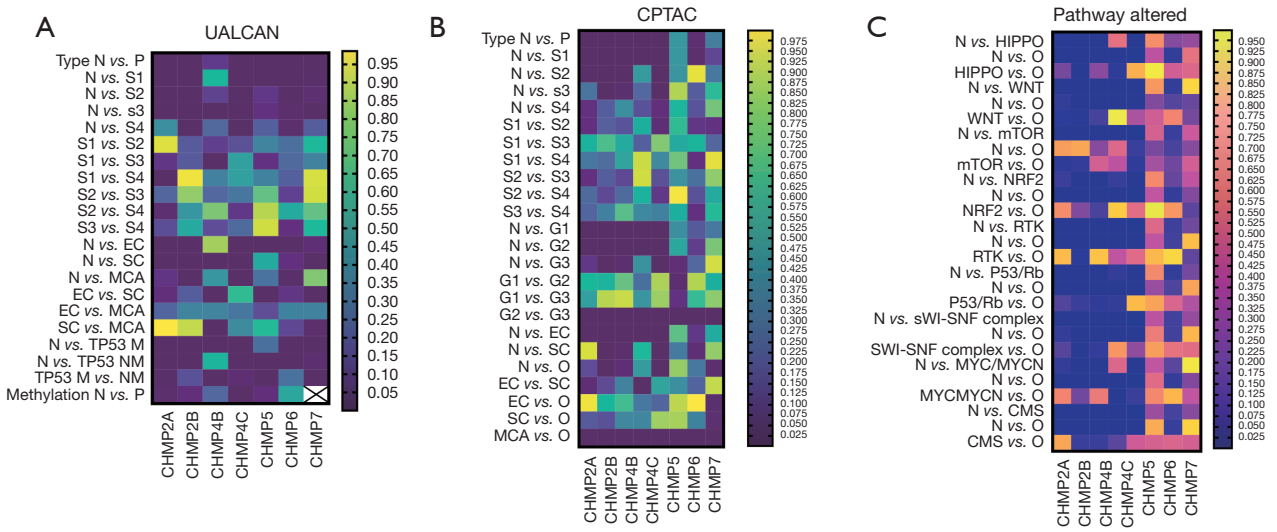

Figure 1 Correlation analysis of the ESCRT pathway genes in clinical pathological characteristics of type, FIGO stage, histological grade, histological subtypes, TP53 mutant, and methylation, which are visualized using the cluster heat maps in (A) UALCAN and (B) CPTAC dataset, and (C) pathway altered. ESCRT, Endosomal Sorting Complex Required for Transport; FIGO, International Federation of Gynecology and Obstetrics; CPTAC, Clinical Proteomic Tumor Analysis Consortium; N, normal; O, others; G, grade, defined as G1, well-differentiated; G2, moderately differentiated; G3, poorly differentiated or undifferentiated; S, stage; EC, endometrioid carcinoma; SC, serous carcinoma; MCA, mixed-cell adenocarcinoma; TP53-M, TP53 mutant; TP53-NM, TP53 non-mutant.

investigate the correlations between the pathway alterations, *CHMP2A*, *CHMP2B*, *CHMP3*, *CHMP4B*, *CHMP4C*, and *CHMP5* were differentially expressed between endometrial cancer tissues (n=100) and normal endometrial tissues (n=31) in HIPPO, WNT, mTOR, NRF2, RTK, P53/Rb, SWI-SNF, MYC/MYCN pathway, and chromatin modifier status. This was determined by conducting the Pearson correlation analysis (*Figure 1B*, Table S4).

TISDIB analysis showed that *CHMP2A*, *CHMP4B*, and *CHMP5* were significantly associated with tumor stage, while *CHMP2A*, *CHMP2B*, *CHMP4B*, *CHMP4C*, *CHMP5*, and *CHMP7* were significantly differentially expressed among different tumor grades. Except for *CHMP7*, all other ESCRT genes were significantly associated with immune subtypes, including wound healing, IFN-gamma dominant, inflammatory, lymphocyte depleted, immunologically quiet, and TGF-b dominant. This was determined by performing the Kruskal-Wallis test (Figure S3). *CHMP2A*, *CHMP4B*, *CHMP5*, and *CHMP7* were significantly associated with a molecular subtype, including POLE (DNA polymerase epsilon), low copy number (CN-LOW), high copy number (CN-HIGH), and microsatellite instability (MSI) (Table S4).

Functional enrichment analysis

GO and KEGG enrichment analyses were performed to determine the biological significance of the genes involved in the ESCRT pathway. Endocytosis (I04144) was the most significantly enriched KEGG pathway analysis, which showed that ESCRT genes were significantly enriched in the endosomal sorting complex required for transport (ESCRT) (hsa917729), membrane trafficking (R-HAS-199991), vesicle-mediated transport (R-HAS-5653656), and macroautophagy (R-HAS-1632852). The main cellular components (CC) were the ESCRT complex (GO:0036452), ESCRT III complex (GO:0000815), endosome membrane (GO:0010008), late endosome (GO:0005770), late endosome membrane (GO:0031902), and endosomal part (GO:0044440).

The GO analysis demonstrated that all the ESCRT pathway genes (*CHMP2A*, *CHMP2B*, *CHMP3*, *CHMP4B*, *CHMP4C*, *CHMP5*, *CHMP5*, and *CHMP7*) were mainly involved in the biological process (BP) of membrane budding (GO:0006900), endosome organization (GO:0007032), endosomal transport (GO:0016197), multivesicular body organization (GO:0036257),

Table 1 ESCRT pathway genes mutation across TCGA project on NIH national cancer institute CDC Data Portal database

	Symbol							
	CHMP2A	CHMP2B	CHMP3	CHMP4B	CHMP4C	CHMP5	CHMP6	CHMP7
Project								
SSM (N=530)								
SSM affected cases	21	26	15	22	14	19	9	36
SSM affected cases in TCGA %	0.0396	0.0491	0.0283	0.0415	0.0264	0.0358	0.017	0.0679
CNV (N=510)								
CNV gains	26	11	8	22	14	21	53	3
CNV gains in TCGA %	0.0510	0.0216	0.0157	0.0431	0.0275	0.0412	0.1039	0.0059
CNV losses	23	23	9	11	5	5	7	32
CNV losses in TCGA %	0.0451	0.0451	0.0176	0.0216	0.0098	0.0098	0.0137	0.0627
All SSM affected cases in UCEC	70	59	32	55	31	45	28	68
Somatic mutation	22	35	16	24	19	22	9	43
Somatic mutation in all SSM affected cases in UCEC %	0.3143	0.5932	0.5	0.4364	0.6129	0.4888	0.3214	0.6324
Disease type								
Adenomas and adenocarcinomas	32	31	18	32	21	26	28	40
Cystic, mucinous and serous neoplasms	38	28	13	23	10	19	0	28
Epithelial neoplasms			1					
Survival								
Dead	13	10	5	10	8	14	16	9
Alive	57	49	27	45	23	31	51	59
Survival rate	0.82	0.72	0.81	0.76	0.68	0.65	0.25	0.84
Interval of last follow-up (Year)	5.095	5.142	5.136	5.106	5.106	5.095	5.008	5.106

ESCRT, endosomal sorting complex required for transport; TCGA, The Cancer Genome Atlas; CNV, copy-number variant; SSM, simple somatic mutation; SNV, single nucleotide variation; UCEC, uterine corpus endometrial carcinoma.

multivesicular body assembly (GO:0036258), multi-organism membrane organization (GO:0044803), and multi-organism membrane budding (GO:1902592), which were related to the main ESCRT function. In addition, *CHMP5* participated in the ESCRT complex assembly (GO:1904895), ESCRT III complex assembly (GO:1904902), *CHMP2A*, *CHMP5*, and *CHMP7*, which participated in the ESCRT complex disassembly (GO:1904896) and ESCRT III complex disassembly (GO:1904903). In addition, *CHMP3* was involved in the regulation of early endosome to late endosome transport (GO:2000641). On the other hand, *CHMP2B*, *CHMP3*, and *CHMP5* were involved in the endosome-to-lysosome transport (GO:0008333). *CHMP3* and *CHMP5* were involved in the multivesicular body sorting pathway (GO:0071985). *CHMP4B* was involved in the protein localization to the membrane (GO:0072657), membrane fission (GO:0090148), and the establishment of protein localization to the membrane (GO:0090150) (*Figure 1C*). Detailed information on the above mentioned involvements is shown in *Table 1*.

The Pearson correlation coefficient analysis results demonstrated that all of the concerned genes enriched

in the ESCRIhsa917729) KEGG pathway in the GEPIA dataset were connected with each other significantly by transcripts per million (TPM) expression values (Figure S4).

ESCRT gene mutations in the EC samples

We observed seven ESCRT pathway genes that were most frequently mutated in the EC samples obtained from the simple somatic mutation (SSM) TCGA cohort (n=530), which included various cancer types, including *CHMP2A* (3.96%), *CHMP2B* (4.91%), *CHMP3* (2.83%), *CHMP4B* (4.15%), *CHMP4C* (2.64%), *CHMP5* (3.58%), and *CHMP7* (6.97%). *CHMP5* (1.70%) was ranked third on the GDC Data Portal (Figure S5). Different mutation categories of the ESCRT genes in the TCGA-UCEC project showed that moderate somatic mutations and missense mutations were the most common types (*Figure 2A*), *CHMP7* ranked most of the various mutations type. Also, *CHMP5* firstly showed CNV gains (*Figure 2B*). Moreover, the ESCRT pathway genes frequently mutated in the modifier of VEP impact mutation (*Figure 2C*), deleterious and tolerated of SIFT impact mutation (*Figure 2D*), probably_damaging and benign of polyphen impact mutation (*Figure 2E*), missense_variant, downstream_gene_variant, 3_prime_UTR_variant of consequence type mutation (*Figure 2F*), single base substitution of type mutation (*Figure 2G*) and somaticsniper mutation (*Figure 2H*) (*Table 2*, Table S3).

ESCRT genes associated with TILs

We explored the correlation between the expression of ESCRT genes and TILs, including 28 distinct immune cell types in the EC samples (n=546) in the TCGA-UCEC database with Spearman correlations using the online tools, TISIDB and GEPIA2021. We found that *CHMP2A*, *CHMP3*, *CHMP4B*, *CHMP5*, *CHMP5*, and *CHMP7* were positively correlated with the infiltration of CD8. *CHMP2B*, *CHMP3*, *CHMP4B*, *CHMP4C*, *CHMP5*, and *CHMP7* were positively correlated with the infiltration of CD4. *CHMP4B*, and *CHMP5* were positively correlated with the infiltration of Tregs. *CHMP3*, *CHMP4B*, and *CHMP5* were positively correlated with the infiltration of NK cells. On the other hand, *CHMP2A* and *CHMP5* were negatively correlated with the infiltration of CD4. *CHMP4C* was negatively correlated with the infiltration of NK and Treg. *CHMP2B* and *CHMP4C* were negatively correlated with the infiltration of CD8, B cells, and macrophages. *CHMP2A*, *CHMP3*, *CHMP5*, and *CHMP7* were negatively correlated with B cells (*Figure 3A,3B*, Table S5). We also detected *CHMP2A* (P=0.0081), *CHMP4B* (P=0.0005), *CHMP4C* (P=0.0002), *CHMP5* (P=0.0231) and *CHMP5* (P=0.0061) were significantly related with TILs (rho value) by multiple liner regression (*Table 3*). Significant differences between the ESCRT genes and TILs were observed in the TCGA-UCEC tumor, normal, and GTEx-uterus datasets in the GEPIA analysis, in which the parameters were grouped by tissue (P<0.05) (*Figure 3C*, Table S5). These results indicate that the *ESCRT-III* pathway genes may be effective markers in EC immunotherapy.

Survival analysis and efficacy evaluation of the ESCRT genes

We performed the Kaplan-Meier survival analysis in UALCAN (Figure S6A). The patients were assigned to high (n=136) or low/medium (n=407) expression groups. The univariate Cox regression analysis in TISIDB (Figure S6B) from the TCGA-UCEC database was used to predict the prognostic values of the ESCRT genes on the OS of patients with EC. The Univariate Cox proportional hazards regression analysis in the GEPIA from TCGA also evaluated OS and DFS in patients with EC. We found that a low expression of *CHMP4B* (log-rank P=0.037) in UALCAN and a high expression of *CHMP2A* in TISDIB (log-rank P=0.0203) had a favorable OS for EC, while high expression of *CHMP2A* [(log-rank) P=0.016, hazard ratio (HR) (high) =0.44, P(HR) =]0.018) and *CHMP7* [(log-rank) P=0.027, HR (high) =0.47, P(HR) =0.03] in GEPIA were positively correlated with a better prognosis of EC (Figure S6C).

In addition, we also performed a survival analysis using the Kaplan-Meier method on the ESCRT mutation genes; the 5-year OS rates/intervals of the last follow-up were as follows: *CHMP2A* (82%, 5.095), *CHMP2B* (72%, 5.142), *CHMP3* (81%, 5.136), *CHMP4B* (76%, 5.106), *CHMP4C* (68%, 5.106), *CHMP5* (65%, 5.095), *CHMP5* (25%, 5.008), and *CHMP7* (84%, 5.106) (Figure S7). The *CHMP5* mutations positively correlated with a spoor prognosis. *CHMP2A*, *CHMP3*, and *CHMP7* mutations demonstrated a good potential for being a prognostic tool in patients with EC (Figure S6, Table S6).

Discussion

Type I EC is associated with microsatellite instability

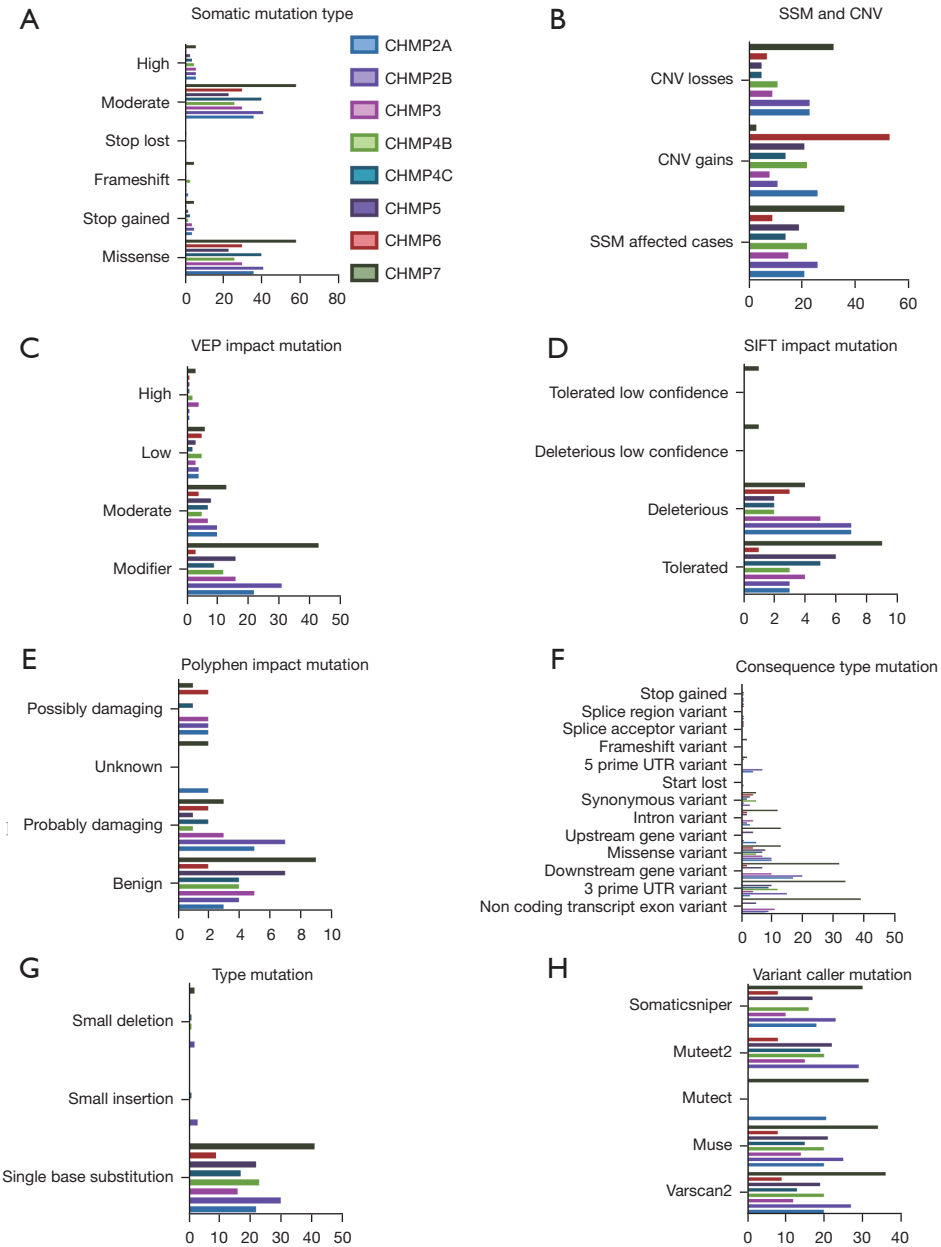

Figure 2 The ESCRT pathway gene mutation types in EC based on the different categories on the TCGA-UCEC database. The tumor mutation burden of each sample is displayed using various colors in the box plots. (A) Somatic mutation; (B) SSM and CNV; (C) VEP impact mutation; (D) SIFT impact mutation; (E) Polyphen impact mutation; (F) consequence type mutation; (G) type mutation; (H) Variant caller mutation. ESCRT, Endosomal Sorting Complex Required for Transport; EC, endometrial carcinoma; TCGA-UCEC, The Cancer Genome Atlas uterine corpus endometrial carcinoma; SSM, simple somatic mutation; CNV, copy-number variant; SNV, single nucleotide variation; VEP, variant effect predictor; SIFT, Sorting Intolerant From Tolerant.

hypermutated (MSI-H) and a copy-number low (CNL) integrated genomic categories in TCGA and frequent mutations in the mTOR pathway (2). Type II EC is characterized by a copy-number high (CN-H) and frequent mutation of TP53 (17). We found that *CHMP2B*, *CHMP3*, *CHMP4B*, *CHMP5*, *CHMP5*, and *CHMP7* were

Table 2 The whole results of GO and KEGG enrichment analysis of the ESCRT genes in EC

Ontology ID	Description	Genes
BP		
GO:0000045	Autophagosome assembly	*CHMP4B*
GO:0000070	Mitotic sister chromatid segregation	*CHMP2A, CHMP2B, CHMP4B, CHMP4C, CHMP5, CHMP6, CHMP7*
GO:0000226	Microtubule cytoskeleton organization	*CHMP2A, CHMP2B, CHMP3, CHMP4B, CHMP4C, CHMP5*
GO:0000281	Mitotic cytokinesis	*CHMP4B,*
GO:0000819	Sister chromatid segregation	*CHMP2A, CHMP2B, CHMP4B, CHMP4C, CHMP5, CHMP6, CHMP7*
GO:0000910	Cytokinesis	*CHMP4B, CHMP4C,*
GO:0000920	Cell separation after cytokinesis	*CHMP2A, CHMP2B, CHMP3, CHMP4B, CHMP4C, CHMP5, CHMP6, CHMP7*
GO:0001881	Receptor recycling	*CHMP5*
GO:0001894	Tissue homeostasis	*CHMP4B*
GO:0001919	Regulation of receptor recycling	*CHMP5*
GO:0006612	Protein targeting to membrane	*CHMP4B*
GO:0006620	Posttranslational protein targeting to membrane	*CHMP4B*
GO:0006887	Exocytosis	*CHMP2A,*
GO:0006900	Membrane budding	*CHMP2A, CHMP2B, CHMP3, CHMP4B, CHMP4C, CHMP5, CHMP6, CHMP7*
GO:0006914	Autophagy	*CHMP2A, CHMP2B, CHMP3, CHMP4B, CHMP4C, CHMP6*
GO:0006997	Nucleus organization	*CHMP2A, CHMP2B, CHMP4B, CHMP4C, CHMP5, CHMP6, CHMP7*
GO:0006998	Nuclear envelope organization	*CHMP2A, CHMP4B, CHMP7*
GO:0007032	Endosome organization	*CHMP2A, CHMP2B, CHMP3, CHMP4B, CHMP4C, CHMP5, CHMP6, CHMP7*
GO:0007033	Vacuole organization	*CHMP2A, CHMP2B, CHMP3, CHMP4B, CHMP4C, CHMP5, CHMP6, CHMP7*
GO:0007034	Vacuolar transport	*CHMP2A, CHMP2B, CHMP3, CHMP4B, CHMP4C, CHMP5, CHMP6, CHMP7*
GO:0007040	Lysosome organization	*CHMP5*
GO:0007041	Lysosomal transport	*CHMP2B, CHMP5*
GO:0007051	Spindle organization	*CHMP2A, CHMP2B, CHMP4B, CHMP4C, CHMP5*
GO:0007059	Chromosome segregation	*CHMP2A, CHMP2B, CHMP4B, CHMP4C, CHMP5, CHMP6, CHMP7*
GO:0007067	Mitotic nuclear division	*CHMP2A, CHMP2B, CHMP4B, CHMP4C, CHMP5, CHMP6, CHMP7*
GO:0007080	Mitotic metaphase plate congression	*CHMP2A, CHMP2B, CHMP4B, CHMP4C, CHMP5, CHMP6, CHMP7*
GO:0007088	Regulation of mitotic nuclear division	*CHMP2A, CHMP2B, CHMP4B, CHMP4C, CHMP5*

Table 2 (*continued*)

Table 2 (*continued*)

Ontology ID	Description	Genes
GO:0007098	Centrosome cycle	*CHMP2A, CHMP2B, CHMP3, CHMP4B, CHMP4C, CHMP5*
GO:0007099	Centriole replication	*CHMP2A*
GO:0007346	Regulation of mitotic cell cycle	*CHMP2A, CHMP2B, CHMP4B, CHMP4C, CHMP5*
GO:0008333	Endosome to lysosome transport	*CHMP2B, CHMP3, CHMP5*
GO:0009838	Abscission	*CHMP4C*
GO:0010324	Membrane invagination	*CHMP2A*
GO:0010458	Exit from mitosis	*CHMP2A, CHMP4B, CHMP7*
GO:0010506	Regulation of autophagy	*CHMP4B*
GO:0010507	Negative regulation of autophagy	*CHMP4B*
GO:0010639	Negative regulation of organelle organization	*CHMP2A, CHMP4B*
GO:0010824	Regulation of centrosome duplication	*CHMP2A, CHMP2B, CHMP3, CHMP4B, CHMP4C, CHMP5*
GO:0010826	Negative regulation of centrosome duplication	*CHMP2A*
GO:0010948	Negative regulation of cell cycle process	*CHMP2A, CHMP4C*
GO:0016050	Vesicle organization	*CHMP2A, CHMP2B, CHMP3, CHMP4B, CHMP4C, CHMP5, CHMP6, CHMP7*
GO:0016197	Endosomal transport	*CHMP2A, CHMP2B, CHMP3, CHMP4B, CHMP4C, CHMP5, CHMP6, CHMP7*
GO:0016236	Macroautophagy	*CHMP3, CHMP4B*
GO:0016241	Regulation of macroautophagy	*CHMP4B*
GO:0016242	Negative regulation of macroautophagy	*CHMP4B*
GO:0016482	Cytosolic transport	*CHMP3*
GO:0017157	Regulation of exocytosis	*CHMP2A*
GO:0019058	Viral life cycle	*CHMP2A, CHMP2B, CHMP3, CHMP4B, CHMP4C, CHMP5, CHMP6, CHMP7*
GO:0019068	Virion assembly	*CHMP2A, CHMP2B, CHMP3, CHMP4B, CHMP4C, CHMP5, CHMP6, CHMP7*
GO:0019076	Viral release from host cell	*CHMP2A, CHMP2B, CHMP3, CHMP4B, CHMP4C*
GO:0031023	Microtubule organizing center organization	*CHMP2A, CHMP2B, CHMP3, CHMP4B, CHMP4C, CHMP5*
GO:0031468	Nuclear envelope reassembly	*CHMP4B, CHMP7*
GO:0032465	Regulation of cytokinesis	*CHMP4C*
GO:0032466	Negative regulation of cytokinesis	*CHMP4C*
GO:0032886	Regulation of microtubule-based process	*CHMP4B, CHMP5*
GO:0032386	Regulation of intracellular transport	*CHMP3*
GO:0032509	Endosome transport via multivesicular body sorting pathway	*CHMP2B, CHMP3*
GO:0032510	Endosome to lysosome transport via multivesicular body sorting pathway	*CHMP2B, CHMP3*

Table 2 (*continued*)

Table 2 (*continued*)

Ontology ID	Description	Genes
GO:0032886	Regulation of microtubule-based process	*CHMP2A, CHMP2B, CHMP3, CHMP4B*
GO:0032984	Macromolecular complex disassembly	*CHMP2A, CHMP2B, CHMP5, CHMP7*
GO:0036257	Multivesicular body organization	*CHMP2A, CHMP2B, CHMP3, CHMP4B, CHMP4C, CHMP5, CHMP6, CHMP7*
GO:0036258	Multivesicular body assembly	*CHMP2A, CHMP2B, CHMP3, CHMP4B, CHMP4C, CHMP5, CHMP6, CHMP7*
GO:0039702	Viral budding via host ESCRT complex	*CHMP2A, CHMP2B, CHMP3, CHMP4B, CHMP4C, CHMP6, CHMP7*
GO:0043112	Receptor metabolic process	*CHMP5*
GO:0043241	Protein complex disassembly	*CHMP2A, CHMP2B, CHMP5, CHMP7*
GO:0043900	Regulation of multi-organism process	*CHMP2A, CHMP2B, CHMP3, CHMP4B, CHMP4C*
GO:0043901	Negative regulation of multi-organism process	*CHMP3*
GO:0043902	Positive regulation of multi-organism process	*CHMP2A, CHMP2B, CHMP3, CHMP4B, CHMP4C*
GO:0043903	Regulation of symbiosis, encompassing mutualism through parasitism	*CHMP2A, CHMP2B, CHMP3, CHMP4B, CHMP4C*
GO:0044770	Cell cycle phase transition	*CHMP2A, CHMP4B, CHMP7*
GO:0044772	Mitotic cell cycle phase transition	*CHMP2A, CHMP4B, CHMP7*
GO:0044801	Single-organism membrane fusion	*CHMP2B, CHMP3*
GO:0044803	Multi-organism membrane organization	*CHMP2A, CHMP2B, CHMP3, CHMP4B, CHMP4C, CHMP5, CHMP6, CHMP7*
GO:0045022	Early endosome to late endosome transport	*CHMP3*
GO:0045047	Protein targeting to ER	*CHMP4B*
GO:0045324	Late endosome to vacuole transport	*CHMP7*
GO:0045786	Negative regulation of cell cycle	*CHMP2A, CHMP4C*
GO:0045921	Positive regulation of exocytosis	*CHMP2A*
GO:0046599	Regulation of centriole replication	*CHMP2A*
GO:0046600	Negative regulation of centriole replication	*CHMP2A*
GO:0046605	Regulation of centrosome cycle	*CHMP2A, CHMP2B, CHMP3, CHMP4B, CHMP4C, CHMP5*
GO:0046606	Negative regulation of centrosome cycle	*CHMP2A*
GO:0046755	Viral budding	*CHMP2A, CHMP2B, CHMP3, CHMP4B, CHMP4C, CHMP5, CHMP6, CHMP7*
GO:0048284	Organelle fusion	*CHMP2B, CHMP3, CHMP4C*
GO:0048524	Positive regulation of viral process	*CHMP2A, CHMP2B, CHMP3, CHMP4B, CHMP4C*
GO:0048871	Multicellular organismal homeostasis	*CHMP4B*
GO:0050000	Chromosome localization	*CHMP2A, CHMP2B, CHMP4B, CHMP4C, CHMP5, CHMP6, CHMP7*
GO:0048525	Negative regulation of viral process	*CHMP3*

Table 2 (*continued*)

Table 2 (*continued*)

Ontology ID	Description	Genes
GO:0050792	Regulation of viral process	*CHMP2A, CHMP2B, CHMP3, CHMP4B, CHMP4C*
GO:0050890	Cognition	*CHMP2B*
GO:0051047	Positive regulation of secretion	*CHMP2A*
GO:0051225	Spindle assembly	*CHMP2A, CHMP2B, CHMP4B, CHMP4C, CHMP5*
GO:0051258	Protein polymerization	*CHMP2A, CHMP3*
GO:0051259	Protein oligomerization	*CHMP2A, CHMP3, CHMP4B*
GO:0051260	Protein homooligomerization	*CHMP2A, CHMP4B*
GO:0051291	Protein heterooligomerization	*CHMP2A, CHMP3*
GO:0051297	Centrosome organization	*CHMP2A, CHMP2B, CHMP3, CHMP4B, CHMP4C, CHMP5*
GO:0051298	Centrosome duplication	*CHMP2A, CHMP2B, CHMP3, CHMP4B, CHMP4C, CHMP5*
GO:0051302	Regulation of cell division	*CHMP4C*
GO:0051303	Establishment of chromosome localization	*CHMP2A, CHMP2B, CHMP4B, CHMP4C, CHMP5, CHMP6, CHMP7*
GO:0051310	Metaphase plate congression	*CHMP2A, CHMP2B, CHMP4B, CHMP4C, CHMP5, CHMP6, CHMP7*
GO:0051493	Regulation of cytoskeleton organization	*CHMP2A, CHMP2B, CHMP3, CHMP4B, CHMP4C, CHMP5*
GO:0051494	Negative regulation of cytoskeleton organization	*CHMP2A*
GO:0060627	Regulation of vesicle-mediated transport	*CHMP3*
GO:0051640	Organelle localization	*CHMP2A, CHMP2B, CHMP4B, CHMP4C, CHMP5, CHMP6, CHMP7*
GO:0051656	Establishment of organelle localization	*CHMP2A, CHMP2B, CHMP4B, CHMP4C, CHMP5, CHMP6, CHMP7*
GO:0051782	Negative regulation of cell division	*CHMP4C*
GO:0051783	Regulation of nuclear division	*CHMP2A, CHMP2B, CHMP4B, CHMP4C, CHMP5*
GO:0060249	Anatomical structure homeostasis	*CHMP2B, CHMP4B*
GO:0060627	Regulation of vesicle-mediated transport	*CHMP2A*
GO:0061025	Membrane fusion	*CHMP2B, CHMP3*
GO:0061511	Centriole elongation	*CHMP2A*
GO:0061763	Multivesicular body-lysosome fusion	*CHMP2B, CHMP3*
GO:0070050	Neuron cellular homeostasis	*CHMP2B*
GO:0070507	Regulation of microtubule cytoskeleton organization	*CHMP2A, CHMP2B, CHMP3, CHMP4B, CHMP4C, CHMP5*
GO:0070972	Protein localization to endoplasmic reticulum	*CHMP4B*
GO:0070997	Neuron death	*CHMP4B*
GO:0071985	Multivesicular body sorting pathway	*CHMP3, CHMP5*
GO:0072599	Establishment of protein localization to endoplasmic reticulum	*CHMP4B*

Table 2 (*continued*)

Table 2 (*continued*)

Ontology ID	Description	Genes
GO:0072657	Protein localization to membrane	*CHMP4B*
GO:0080171	Lytic vacuole organization	*CHMP5*
GO:0090148	Membrane fission	*CHMP4B*
GO:0090150	Establishment of protein localization to membrane	*CHMP4B*
GO:0090169	Regulation of spindle assembly	*CHMP2A, CHMP2B, CHMP4B, CHMP4C, CHMP5*
GO:0090174	Organelle membrane fusion	*CHMP2B, CHMP3*
GO:0090224	Regulation of spindle organization	*CHMP2A, CHMP2B, CHMP4B, CHMP4C, CHMP5*
GO:0090307	Mitotic spindle assembly	*CHMP2A, CHMP2B, CHMP4B, CHMP4C, CHMP5*
GO:0090611	Ubiquitin-independent protein catabolic process via the multivesicular body sorting pathway	*CHMP4B, CHMP4C*
GO:0097352	Autophagosome maturation	*CHMP3*
GO:0097576	Vacuole fusion	*CHMP2B, CHMP3*
GO:0098534	Centriole assembly	*CHMP2A*
GO:0098813	Nuclear chromosome segregation	*CHMP2A, CHMP2B, CHMP4B, CHMP4C, CHMP5, CHMP6, CHMP7*
GO:0098927	Vesicle-mediated transport between endosomal compartments	*CHMP3*
GO:1901673	Regulation of mitotic spindle assembly	*CHMP2A, CHMP2B, CHMP4C, CHMP5*
GO:1901214	Regulation of neuron death	*CHMP4B*
GO:1902115	Regulation of organelle assembly	*CHMP2A, CHMP2B, CHMP4B, CHMP4C, CHMP5*
GO:1902116	Negative regulation of organelle assembly	*CHMP2A, CHMP4B*
GO:1902186	Regulation of viral release from host cell	*CHMP2A, CHMP2B, CHMP3, CHMP4B, CHMP4C*
GO:1902187	Negative regulation of viral release from host cell	*CHMP3*
GO:1902188	Positive regulation of viral release from host cell	*CHMP2A, CHMP2B, CHMP3, CHMP4B, CHMP4C*
GO:1902590	Multi-organism organelle organization	*CHMP2A, CHMP2B, CHMP3, CHMP4B, CHMP4C, CHMP5, CHMP6, CHMP7*
GO:1902592	Multi-organism membrane budding	*CHMP2A, CHMP2B, CHMP3, CHMP4B, CHMP4C, CHMP5, CHMP6, CHMP7*
GO:1903335	Regulation of vacuolar transport	*CHMP3*
GO:1903649	Regulation of cytoplasmic transport	*CHMP3*
GO:1902850	Microtubule cytoskeleton organization involved in mitosis	*CHMP2A, CHMP2B, CHMP4B, CHMP4C, CHMP5*
GO:1903532	Positive regulation of secretion by cell	*CHMP2A*
GO:1903541	Regulation of exosomal secretion	*CHMP2A*
GO:1903543	Positive regulation of exosomal secretion	*CHMP2A*
GO:1903722	Regulation of centriole elongation	*CHMP2A*
GO:1903723	Negative regulation of centriole elongation	*CHMP2A*

Table 2 (*continued*)

Table 2 (*continued*)

Ontology ID	Description	Genes
GO:1903900	Regulation of viral life cycle	*CHMP2A, CHMP2B, CHMP3, CHMP4C*
GO:1903901	Negative regulation of viral life cycle	*CHMP3*
GO:1903902	Positive regulation of viral life cycle	*CHMP2A, CHMP2B, CHMP3, CHMP4B, CHMP4C*
GO:1904895	ESCRT complex assembly	*CHMP6*
GO:1904896	ESCRT complex disassembly	*CHMP2A, CHMP5, CHMP7*
GO:1904902	ESCRT III complex assembly	*CHMP6*
GO:1904903	ESCRT III complex disassembly	*CHMP2A, CHMP5, CHMP7*
GO:1905037	Autophagosome organization	*CHMP4B*
GO:1990182	Exosomal secretion	*CHMP2A*
GO:2000641	Regulation of early endosome to late endosome transport	*CHMP3*
GO:2000785	Regulation of autophagosome assembly	*CHMP4B*
MF		
GO:0002020	Protease binding	*CHMP3*
GO:0031210	Phosphatidylcholine binding	*CHMP2A, CHMP3*
GO:0045296	Cadherin binding	*CHMP2B, CHMP4B, CHMP5*
GO:0047485	Protein N-terminus binding	*CHMP6*
GO:0050839	Cell adhesion molecule binding	*CHMP2B, CHMP4B, CHMP5*
GO:0008565	Protein transporter activity	*CHMP7*
GO:0098631	Protein binding involved in cell adhesion	*CHMP2B, CHMP4B, CHMP5*
GO:0098632	Protein binding involved in cell-cell adhesion	*CHMP2B, CHMP4B, CHMP5*
GO:0098641	Cadherin binding involved in cell-cell adhesion	*CHMP2B, CHMP4B, CHMP5*
GO:0070405	Ammonium ion binding	*CHMP2A, CHMP3*
GO:1990381	Ubiquitin-specific protease binding	*CHMP3*
CC		
GO:000815	ESCRT III complex	*CHMP2A, CHMP2B, CHMP3, CHMP4B, CHMP4C, CHMP6, CHMP7*
GO:0005635	Nuclear envelope	*CHMP2A, CHMP4B, CHMP7*
GO:0005770	Late endosome	*CHMP2A, CHMP2B, CHMP3, CHMP4B, CHMP4C, CHMP6*
GO:0005913	Cell-cell adherens junction	*CHMP5*
GO:0010008	Endosome membrane	*CHMP2A, CHMP2B, CHMP3, CHMP4C, CHMP5, CHMP6, CHMP7*
GO:0030117	Membrane coat	*CHMP2A*
GO:0030496	Midbody	*CHMP4C*
GO:0031902	Late endosome membrane	*CHMP2A, CHMP2B, CHMP3, CHMP4C, CHMP6*
GO:0036452	ESCRT complex	*CHMP2A, CHMP2B, CHMP3, CHMP4C, CHMP6, CHMP7*

Table 2 (*continued*)

Table 2 (*continued*)

Ontology ID	Description	Genes
GO:0044440	Endosomal part	*CHMP2A, CHMP2B, CHMP3, CHMP4B, CHMP4C, CHMP5, CHMP7*
GO:0048475	Coated membrane	*CHMP2A, CHMP4B*
GO:0090543	Flemming body	*CHMP4C*
GO:0098552	Side of membrane	*CHMP4B*
GO:0098562	Cytoplasmic side of membrane	*CHMP4B*
KEGG pathway		
Hsa04144	Endocytosis	*CHMP2A, CHMP2B, CHMP3, CHMP4B, CHMP4C, CHMP5*
Reactome pathway		
R-HAS-162588	Budding and maturation of HIV virion	*CHMP2A, CHMP2B, CHMP3, CHMP4B, CHMP4C, CHMP5, CHMP6, CHMP7*
R-HAS-2262752	Cellular responses to stress	*CHMP2A, CHMP2B, CHMP3, CHMP4B, CHMP4C, CHMP6, CHMP7*
R-HAS-421837	Clathrin derived vesicle budding	*CHMP2A*
R-HAS-1643685	Disease	*CHMP2A, CHMP2B, CHMP3, CHMP4B, CHMP4C, CHMP5, CHMP6, CHMP7*
R-HAS-917729	Endosomal Sorting Complex Required For Transport (ESCRT)	*CHMP2A, CHMP2B, CHMP3, CHMP4B, CHMP4C, CHMP5, CHMP6, CHMP7*
R-HAS-162906	HIV Infection	*CHMP2A, CHMP2B, CHMP3, CHMP4B, CHMP4C, CHMP5, CHMP6, CHMP7*
R-HAS-162587	HIV Life Cycle	*CHMP2A, CHMP2B, CHMP3, CHMP4B, CHMP4C, CHMP5, CHMP6, CHMP7*
R-HAS-5663205	Infectious disease	*CHMP2A, CHMP2B, CHMP3, CHMP4B, CHMP4C, CHMP5, CHMP6, CHMP7*
R-HAS-162599	Late Phase of HIV Life Cycle	*CHMP2A, CHMP2B, CHMP3, CHMP4B, CHMP4C, CHMP5, CHMP6, CHMP7*
R-HAS-432720	Lysosome Vesicle Biogenesis	*CHMP2A*
R-HAS-1632852	Macroautophagy	*CHMP2A, CHMP2B, CHMP3, CHMP4B, CHMP4C, CHMP6, CHMP7*
R-HAS-199991	Membrane Trafficking	*CHMP2A, CHMP2B, CHMP3, CHMP4B, CHMP4C, CHMP5, CHMP6, CHMP7*
R-HAS-5653656	Vesicle-mediated transport	*CHMP2A, CHMP2B, CHMP3, CHMP4B, CHMP4C, CHMP5, CHMP6, CHMP7*
R-HAS-199992	Trans-Golgi Network Vesicle Budding	*CHMP2A*

BP, biological process; CC, cellular component; ESCRT, MF, molecular function; GO, Gene Ontology; KEGG, Kyoto Encyclopedia of Genes; ER,endoplasmic reticulum; HIV, human immunodeficiency virus.

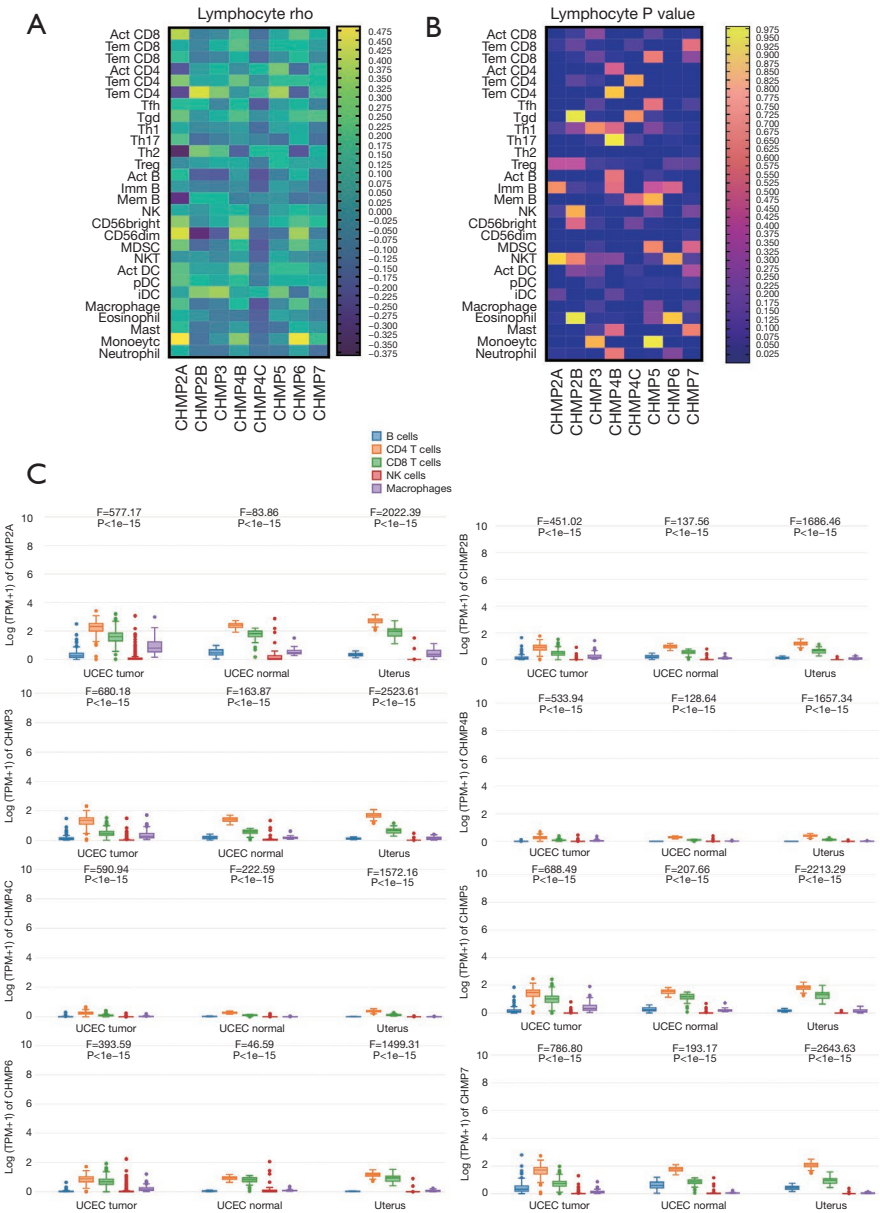

Figure 3 Relationship between the abundance of TILs and gene expression. This was determined via conducting the Spearman correlation in the EC sample on the TCGA-UCEC database in the TISDB analysis. The stacked bar graph shows the infiltration of 28 immune cells in each sample. Each color represents a rho (A) or P value (B) in a type of immune cell. The X axis represents the association between the ESCRT pathway gene expression and immune subtypes across UCEC. The Y axis represents the TIL abundance Kruskal-Wallis Test (–log 10pv). (A) Rho in Lymphocyte; (B) P value in Lymphocyte; (C) the difference between the ESCRT genes: *CHMP2A*, *CHMP2B*, *CHMP3*, *CHMP4B*, *CHMP4C*, *CHMP5*, *CHMP5*, *CHMP7* and TILs on TCGA-UCEC tumor, normal and GTEx-Uterus dataset. The Y axis represents log (TPM+1) in GEPIA analysis. UCEC, uterine corpus endometrial carcinoma; TPM, transcripts per million; TILs, tumor-infiltrating immune cells; Act CD8, activated CD8 T cell; Tcm CD8, central memory CD8 T cell; Tem CD8, effector memory CD8 T cell; Act CD4, Activated CD4 T cell; Tcm CD4, central memory CD4 T cell; Tem CD4, Effector memory CD4 T cell; Tfh, T follicular helper cell; Tgd, gamma delta T cell; Th1, type 1 T helper cell; Th17, type 17 T helper cell; Th2, type 2 T helper cell; Treg, regulatory T cell; Act B, activated B cell; Imm B, immature B cell; Mem B, memory B cell; NK, natural killer cell; CD56bright, CD56bright natural killer cell; CD56dim, CD56dim natural killed cell; MDSC, myeloid derived suppressor cell; NKT, natural killer T cell; Act DC, activated dendritic cell; pDC, plasmacytoid dendritic cell; iDC, immature dendritic cell.

Table 3 Relationship between TILs (rho value) and ESCRT genes by multiple liner regression

Model	CHMP2A	CHMP2B	CHMP3	CHMP4B	CHMP4C	CHMP5	CHMP6	CHMP7
Parameter estimates	0.1175	–0.002861	0.01904	0.1020	–0.09654	0.05768	0.09136	0.01939
Standard error	0.04108	0.03143	0.02620	0.02584	0.02275	0.02394	0.03072	0.02259
95% CI	0.03321 to 0.2018	–0.06735 to 0.06163	–0.03473 to 0.07280	0.04903 to 0.1550	–0.1432 to –0.04985	0.008554 to 0.1068	0.02832 to 0.1544	–0.02697 to 0.06575
[t]	2.860	0.09102	0.7264	3.950	4.243	2.409	2.974	0.8583
P value	0.0081	0.9281	0.4738	0.0005	0.0002	0.0231	0.0061	0.3983

TILs, tumor-infiltrating immune cells; ESCRT, endosomal sorting complex required for transport; CI, confidence interval.

significantly lower, whereas *CHMP2A* and *CHMP4C* were significantly higher in EC samples than in normal tissues. Since histological grade and clinical stage greatly affected the prognosis prediction of EC (1), we explored it found that all of the ESCRT pathway genes were significantly differentially expressed between grades 2 and 3. Increased expression of *CHMP2A* and *CHMP7* and decreased expression of *CHMP4B* were related to endometrioid carcinoma samples compared with serous carcinoma samples. Furthermore, the results of the survival analysis revealed that upregulation of *CHMP2A* and *CHMP7* and downregulation of *CHMP4B* corresponded to a good prognosis in patients with EC. All three genes were significantly associated with all four molecular subtypes in TCGA. Therefore, we indicated that high levels of *CHMP2A* and *CHMP7* and low levels of *CHMP4B* were associated with good prognostic tumor type and early grade and were effective indicators of good prognosis in EC. *CHMP2A*, *CHMP2B*, *CHMP3*, *CHMP4B*, *CHMP4C*, and *CHMP5* were significantly correlated with HIPPO, WNT, mTOR, NRF2, RTK, P53/Rb, SWI-SNF, MYC/MYCN pathway, and chromatin modifier status in EC tissues. As such, temsirolimus and everolimus, which are mTOR inhibitors, are effective in the treatment of recurrent chemotherapy (18,19). Moreover, *ESCRT-III* genes are effective markers for targeted therapy.

We found that most of the ESCRT pathway genes were frequently mutated in EC samples compared with the other cancer types obtained from the TCGA cohort. Additionally, missense mutations were the most common type of mutation. *CHMP7* was the first modifier of VEP impact mutation, which was deleterious and tolerated by the SIFT Impact Mutation. Mutations in *CHMP2A* and *CHMP7* had a good prognostic potential in EC. Dysfunction of ESCRT was associated with cancer, myopathy, and neurodegeneration. Missense mutations in *CHMP4B* were associated with posterior subcapsular or polar cataracts (20-22). Other studies showed that *CHMP2B* mutations that were linked to defects in the process of dissociation from ESCRT disrupted endosome-to-lysosome trafficking, degradation, and recycling. Thus, this resulted in defective mitochondria, imbalanced iron homeostasis, reactive oxygen species, neuronal damage (23,24), endocytic and autophagic defects (25-27) in autosomal dominant presenile dementia (28), amyotrophic lateral sclerosis, cortical basal degeneration (CBD) or familial frontotemporal lobar degeneration (FTLD) and frontotemporal dementia (FTD) (29).

The results of functional analysis revealed that the endocytosis and ESCRT was the most significantly enriched KEGG and Reactome pathways associated with the ESCRT genes in ECs. All concerned ESCRT pathway genes were mainly involved in the BPs of membrane budding, multivesicular body organization, and assembly. The main related CC were the ESCRT and ESCRT III complex. The latter was involved in transmembrane protein delivery and in the promotion of nuclear envelope sealing and mitotic spindle disassembly during the late endosome anaphase (30). Protein sorting from the endosome to the vacuole/lysosome transportation and degradation in eukaryotic cells required the formation of MVBs, which, in turn, required the sequential functioning of ESCRT, -I, -II, and -III complexes in four steps: cargo recognition and sorting, which was initiated by the binding of ESCRT-0 to the Phosphatidyl inositol 3-phosphate (PI3P) on endosomes; cargo sequestration, in which ESCRT-0 recruited ESCRT-I and interacted with ESCRT-II and -III; MVB vesicle formation, in which *ESCRT-III* proteins dissociated and assembled; and the ESCRT disassembly, in which the final step of the MVB pathway was formed (31-33). *CHMP5* served as an acceptor for the ESCRT-II complex on the endosomal membranes

in the *ESCRT-III* complex, thus participating in ESCRT and ESCRT III complex assembly in BP, while *CHMP2A*, *CHMP5*, and *CHMP7* participated in the BP of ESCRT and ESCRT III complex disassembly. In the late stages of cytokinesis, *CHMP3* was responsible for endosomal sorting/trafficking of the EGF receptor. *CHMP4C* was a key component of the cytokinesis checkpoint that delayed abscission and prevented both premature chromosome bridges of the cells and the accumulation of DNA damages (34,35). *CHMP2B*, *CHMP3*, and *CHMP5* were involved in the BP of the multivesicular body sorting pathways and the regulation of early to late endosome transport. All of the key genes were significantly and positively correlated with each other, revealing that the ESCRT pathway might also be involved in the mechanism of the MVB pathway in EC.

On the other hand, tumor-infiltrating immune cells (TICs) modulated cancer cell functions in the tumor microenvironment (36). This could be a basis for immunotherapy, in which the endogenous immune response against tumor cells would be stimulated. Furthermore, this could be associated with the prognosis of patients with EC. ECs stimulate immune checkpoints and activate negative feedback mechanisms in a locally immunosuppressed environment to evade the immune system (37). Memory CD4+ T cells, activated NK cells, and dendritic cells all decreased with an increase in EC grade and stage, which was related to the occurrence of EC. However, high levels of Tregs indicate a good prognosis (38). Our preliminary results show strong correlations between all ESCRT genes and infiltration levels of multiple immune cell types in EC samples. *CHMP2A* and *CHMP7* were positively correlated with the infiltration of CD4 and negatively correlated with B cells, while *CHMP4B* was associated with the infiltration of CD4, CD8, Treg, and NK cells. These three genes may potentially be immune-related indicators for the prognosis of EC and may become the basis for EC immunotherapies.

It has been found that EC cells represent the highest activated programmed death receptor-1 (PD1)/PD-L1expression in endometrioid endometrial adenocarcinoma (EEC), serous endometrial adenocarcinoma (ESC), and clear cell subtypes for 40–80%, 10–68%, and 23–69%, respectively. On the other hand, inactivate tumor-infiltrating CD4 and CD8 T cells are found in the tumor microenvironment (39). Targeting the PD1 pathway may be a great strategy in enhancing the antitumor immune response for EC treatment. Anti-PD-L1 antibodies, such as pembrolizumab, nivolumab, and atezolizumab, have been proven clinically effective in tumors with mismatch-repair deficiency in EC patients in clinical trials, with a 13–48% ORR, 19.0% PFS, and 68.8% OS rates (40-44). Pembrolizumab is an immune checkpoint blockade anti-PD1 antibody that has been used in patients with POLE-mutated (43) and MMR-deficient endometrial cancer (45). We observed that, except for *CHMP7*, all other ESCRT genes were significantly associated with the immune subtype. *CHMP2A*, *CHMP4B*, *CHMP5*, and *CHMP7* were significantly associated with the POLE-mutated molecular subtype in TCGA, which was identified in 10% of endometrioid subtypes. Therefore, elucidation of *CHMP2A*, *CHMP4B*, *CHMP7*, and immune cell interplay would assist in the prediction of immunotherapy responses and development of novel immunotherapy targets.

Conclusions

Our present study confirmed that RNA expression data on multiple datasets showed the relationship between *ESCRT-III* genes and EC. *ESCRT-III* genes may be used as clinical biomarkers for the prognostic prediction and immunotherapy strategies in patients with EC. Further research should be conducted to determine the mechanisms of ESCRT genes as biomarkers and therapeutic targets for the treatment of EC.

Acknowledgments

We thank Elsevier Author Servives (https://webshop.elsevier.com/language-editing-services/language-editing/) for its linguistic assistance during the preparation of this manuscript.

Funding: This work was supported by National Natural Science Foundation of China (Nos. 81902628, 81900036), Translational Medicine Cross Research Fund of Shanghai Jiao Tong University School of Medicine (No. ZH2018QNB08), Clinical Research Project of Shanghai Health Commission (No. 202040455) and Shanghai Songjiang District Science and Technology Research (Medical and Health) Project (Nos. 20SJKJGG139, 20SJKJGG304).

Footnote

Reporting Checklist: The authors have completed the STREGA reporting checklist. Available at https://tcr.

amegroups.com/article/view/10.21037/tcr-22-660/rc

Peer Review File: Available at https://tcr.amegroups.com/article/view/10.21037/tcr-22-660/prf

Conflicts of Interest: Both authors have completed the ICMJE uniform disclosure form (available at https://tcr.amegroups.com/article/view/10.21037/tcr-22-660/coif). The authors have no conflicts of interest to declare.

Ethical Statement: The authors are accountable for all aspects of the work in ensuring that questions related to the accuracy or integrity of any part of the work are appropriately investigated and resolved. This study conformed to the provisions of the Declaration of Helsinki (as revised in 2013).

References

1. Siegel RL, Miller KD, Fuchs HE, et al. Cancer statistics, 2022. CA Cancer J Clin 2022;72:7-33.
2. Bokhman JV. Two pathogenetic types of endometrial carcinoma. Gynecol Oncol 1983;15:10-7.
3. Connor EV, Rose PG. Management Strategies for Recurrent Endometrial Cancer. Expert Rev Anticancer Ther 2018;18:873-85.
4. Ribas A, Wolchok JD. Cancer immunotherapy using checkpoint blockade. Science 2018;359:1350-5.
5. Gong YN, Guy C, Olauson H, et al. *ESCRT-III* Acts Downstream of MLKL to Regulate Necroptotic Cell Death and Its Consequences. Cell 2017;169:286-300.e16.
6. Rühl S, Shkarina K, Demarco B, et al. ESCRT-dependent membrane repair negatively regulates pyroptosis downstream of GSDMD activation. Science 2018;362:956-60.
7. Dai E, Meng L, Kang R, et al. *ESCRT-III*-dependent membrane repair blocks ferroptosis. Biochem Biophys Res Commun 2020;522:415-21.
8. McCullough J, Frost A, Sundquist WI. Structures, Functions, and Dynamics of *ESCRT-III*/Vps4 Membrane Remodeling and Fission Complexes. Annu Rev Cell Dev Biol 2018;34:85-109.
9. Liu J, Kang R, Tang D. *ESCRT-III*-mediated membrane repair in cell death and tumor resistance. Cancer Gene Ther 2021;28:1-4.
10. Chandrashekar DS, Bashel B, Balasubramanya SAH, et al. UALCAN: A Portal for Facilitating Tumor Subgroup Gene Expression and Survival Analyses. Neoplasia 2017;19:649-58.
11. Zhong X, Liu Y, Liu H, et al. Identification of Potential Prognostic Genes for Neuroblastoma. Front Genet 2018;9:589.
12. Tang Z, Li C, Kang B, et al. GEPIA: a web server for cancer and normal gene expression profiling and interactive analyses. Nucleic Acids Res 2017;45:W98-W102.
13. Chen F, Chandrashekar DS, Varambally S, et al. Pan-cancer molecular subtypes revealed by mass-spectrometry-based proteomic characterization of more than 500 human cancers. Nat Commun 2019;10:5679.
14. Ru B, Wong CN, Tong Y, et al. TISIDB: an integrated repository portal for tumor-immune system interactions. Bioinformatics 2019;35:4200-2.
15. Charoentong P, Finotello F, Angelova M, et al. Pan-cancer Immunogenomic Analyses Reveal Genotype-Immunophenotype Relationships and Predictors of Response to Checkpoint Blockade. Cell Rep 2017;18:248-62.
16. Hänzelmann S, Castelo R, Guinney J. GSVA: gene set variation analysis for microarray and RNA-seq data. BMC Bioinformatics 2013;14:7.
17. Cancer Genome Atlas Research Network; Kandoth C, Schultz N, et al. Integrated genomic characterization of endometrial carcinoma. Nature 2013;497:67-73.
18. Oza AM, Elit L, Tsao MS, et al. Phase II study of temsirolimus in women with recurrent or metastatic endometrial cancer: a trial of the NCIC Clinical Trials Group. J Clin Oncol 2011;29:3278-85.
19. Slomovitz BM, Lu KH, Johnston T, et al. A phase 2 study of the oral mammalian target of rapamycin inhibitor, everolimus, in patients with recurrent endometrial carcinoma. Cancer 2010;116:5415-9.
20. Zhang XH, Da Wang J, Jia HY, et al. Mutation profiles of congenital cataract genes in 21 northern Chinese families. Mol Vis 2018;24:471-7.
21. Shiels A, Bennett TM, Knopf HL, et al. *CHMP4B*, a novel gene for autosomal dominant cataracts linked to chromosome 20q. Am J Hum Genet 2007;81:596-606.
22. Wang X, Wang D, Wang Q, et al. Broadening the

Mutation Spectrum in GJA8 and *CHMP4B*: Novel Missense Variants and the Associated Phenotypes in Six Chinese Han Congenital Cataracts Families. Front Med (Lausanne) 2021;8:713284.
23. Zhang Y, Schmid B, Nikolaisen NK, et al. Patient iPSC-Derived Neurons for Disease Modeling of Frontotemporal Dementia with Mutation in *CHMP2B*. Stem Cell Reports 2017;8:648-58.
24. Han JH, Ryu HH, Jun MH, et al. The functional analysis of the *CHMP2B* missense mutation associated with neurodegenerative diseases in the endo-lysosomal pathway. Biochem Biophys Res Commun 2012;421:544-9.
25. Filimonenko M, Stuffers S, Raiborg C, et al. Functional multivesicular bodies are required for autophagic clearance of protein aggregates associated with neurodegenerative disease. J Cell Biol 2007;179:485-500.
26. Isaacs AM, Johannsen P, Holm I, et al. Frontotemporal dementia caused by *CHMP2B* mutations. Curr Alzheimer Res 2011;8:246-51.
27. Lu Y, Zhang Z, Sun D, et al. Syntaxin 13, a genetic modifier of mutant *CHMP2B* in frontotemporal dementia, is required for autophagosome maturation. Mol Cell 2013;52:264-71.
28. Skibinski G, Parkinson NJ, Brown JM, et al. Mutations in the endosomal ESCRTIII-complex subunit *CHMP2B* in frontotemporal dementia. Nat Genet 2005;37:806-8.
29. Toft A, Roos P, Jääskeläinen O, et al. Serum Neurofilament Light in Patients with Frontotemporal Dementia Caused by *CHMP2B* Mutation. Dement Geriatr Cogn Disord 2020;49:533-8.
30. Schöneberg J, Lee IH, Iwasa JH, et al. Reverse-topology membrane scission by the ESCRT proteins. Nat Rev Mol Cell Biol 2017;18:5-17.
31. Mierzwa BE, Chiaruttini N, Redondo-Morata L, et al. Dynamic subunit turnover in *ESCRT-III* assemblies is regulated by Vps4 to mediate membrane remodelling during cytokinesis. Nat Cell Biol 2017;19:787-98.
32. Schöneberg J, Pavlin MR, Yan S, et al. ATP-dependent force generation and membrane scission by *ESCRT-III* and Vps4. Science 2018;362:1423-8.
33. Maity S, Caillat C, Miguet N, et al. VPS4 triggers constriction and cleavage of *ESCRT-III* helical filaments. Sci Adv 2019;5:eaau7198.
34. Liu B, Guo S, Li GH, et al. *CHMP4C* regulates lung squamous carcinogenesis and progression through cell cycle pathway. J Thorac Dis 2021;13:4762-74.
35. Neggers JE, Paolella BR, Asfaw A, et al. Synthetic Lethal Interaction between the ESCRT Paralog Enzymes VPS4A and VPS4B in Cancers Harboring Loss of Chromosome 18q or 16q. Cell Rep 2020;33:108493.
36. Costa AC, Santos JMO, Gil da Costa RM, et al. Impact of immune cells on the hallmarks of cancer: A literature review. Crit Rev Oncol Hematol 2021;168:103541.
37. Di Tucci C, Capone C, Galati G, et al. Immunotherapy in endometrial cancer: new scenarios on the horizon. J Gynecol Oncol 2019;30:e46.
38. Chen B, Wang D, Li J, et al. Screening and Identification of Prognostic Tumor-Infiltrating Immune Cells and Genes of Endometrioid Endometrial Adenocarcinoma: Based on The Cancer Genome Atlas Database and Bioinformatics. Front Oncol 2020;10:554214.
39. Herzog TJ, Arguello D, Reddy SK, et al. PD-1, PD-L1 expression in 1599 gynecological cancers: Implications for immunotherapy. Gynecol Oncol. 2015;137:204-5.
40. Le DT, Uram JN, Wang H, et al. PD-1 Blockade in Tumors with Mismatch-Repair Deficiency. N Engl J Med 2015;372:2509-20.
41. Ott PA, Bang YJ, Berton-Rigaud D, et al. Safety and Antitumor Activity of Pembrolizumab in Advanced Programmed Death Ligand 1-Positive Endometrial Cancer: Results From the KEYNOTE-028 Study. J Clin Oncol 2017;35:2535-41.
42. Makker V, Rasco DW, Dutcus CE, et al. A phase Ib/II trial of lenvatinib (LEN) plus pembrolizumab (Pembro) in patients (Pts) with endometrial carcinoma. J Clin Oncol 2017;35:5598.
43. Mehnert JM, Panda A, Zhong H, et al. Immune activation and response to pembrolizumab in POLE-mutant endometrial cancer. J Clin Invest 2016;126:2334-40.
44. Santin AD, Bellone S, Buza N, et al. Regression of Chemotherapy-Resistant Polymerase ε (POLE) Ultra-Mutated and MSH6 Hyper-Mutated Endometrial Tumors with Nivolumab. Clin Cancer Res 2016;22:5682-7.
45. Le DT, Durham JN, Smith KN, et al. Mismatch repair deficiency predicts response of solid tumors to PD-1 blockade. Science 2017;357:409-13.

Cite this article as: Yang Y, Wang M. Genomic analysis of the endosomal sorting required for transport complex III pathway genes as therapeutic and prognostic biomarkers for endometrial carcinoma. Transl Cancer Res 2022;11(9):3108-3127. doi: 10.21037/tcr-22-660

